JGS
Journal of the Geological Society

Research article

Published Online First

https://doi.org/10.1144/jgs2021-036

The grandest of them all: the Lomagundi–Jatuli Event and Earth's oxygenation

A.R. Prave[1]*, K. Kirsimäe[2], A. Lepland[2,3], A.E. Fallick[4], T. Kreitsmann[2], Yu.E. Deines[5], A.E. Romashkin[5]†, D.V. Rychanchik[5], P.V. Medvedev[5], M. Moussavou[6], K. Bakakas[6] and M.S.W. Hodgskiss[7]

[1] School of Earth and Environmental Sciences, University of St Andrews, St Andrews KY16 9AL, UK
[2] Department of Geology, University of Tartu, Tartu 50411, Estonia
[3] Geological Survey of Norway, Trondheim 7491, Norway
[4] SUERC, Rankine Avenue, East Kilbride G75 0QF, UK
[5] Institute of Geology, Karelian Research Centre, Russian Academy of Sciences, Pushkinskaya 11, Petrozavodsk 185610, Russia
[6] Department of Geology, Université des Sciences et Techniques de Masuku, 943, Franceville, Gabon
[7] Department of Earth Sciences, University of Cambridge, Cambridge CB2 3EQ, UK

ARP, 0000-0002-4614-3774; AEF, 0000-0002-7649-6167; YED, 0000-0002-9574-1893; PVM, 0000-0002-4098-5321; KB, 0000-0002-6061-005X; MSWH, 0000-0001-8859-2765

* Correspondence: ap13@st-andrews.ac.uk

† Deceased, and to whom we dedicate this work

Abstract: The Paleoproterozoic Lomagundi–Jatuli Event (LJE) is generally considered the largest, in both amplitude and duration, positive carbonate C-isotope ($\delta^{13}C_{carb}$) excursion in Earth history. Conventional thinking is that it represents a global perturbation of the carbon cycle between 2.3–2.1 Ga linked directly with, and in part causing, the postulated rise in atmospheric oxygen during the Great Oxidation Event. In addition to new high-resolution $\delta^{13}C_{carb}$ measurements from LJE-bearing successions of NW Russia, we compiled 14 943 $\delta^{13}C_{carb}$ values obtained from marine carbonate rocks 3.0–1.0 Ga in age and from selected Phanerozoic time intervals as a comparator of the LJE. Those data integrated with sedimentology show that, contra to consensus, the $\delta^{13}C_{carb}$ trend of the LJE is facies (i.e. palaeoenvironment) dependent. Throughout the LJE interval, the C-isotope composition of open and deeper marine settings maintained a mean $\delta^{13}C_{carb}$ value of +1.5 ± 2.4‰, comparable to those settings for most of Earth history. In contrast, the ^{13}C-rich values that are the hallmark of the LJE are limited largely to nearshore-marine and coastal-evaporitic settings with mean $\delta^{13}C_{carb}$ values of +6.2 ± 2.0‰ and +8.1 ± 3.8‰, respectively. Our findings confirm that changes in $\delta^{13}C_{carb}$ are linked directly to facies changes and archive *contemporaneous* dissolved inorganic carbon pools having variable C-isotopic compositions in laterally adjacent depositional settings. The implications are that the LJE cannot be construed *a priori* as representative of the global carbon cycle or a planetary-scale disturbance to that cycle, nor as direct evidence for oxygenation of the ocean–atmosphere system. This requires rethinking models relying on those concepts and framing new ideas in the search for understanding the genesis of the grandest of all positive C-isotope excursions, its timing and its hypothesized linkage to oxygenation of the atmosphere.

Supplementary material: C–O isotope data, figure S1, tables S1–S5 and the dataset for $\delta^{13}C_{carb}$ values are available at https://doi.org/10.6084/m9.figshare.c.5471815

Received 11 March 2021; **revised** 11 June 2021; **accepted** 17 June 2021

Evidence of the oxygenation of Earth's surface environments during the Paleoproterozoic is based on a now familiar list of temporally linked phenomena that includes geological features (decline of banded-iron formation, cessation of uraninite and pyrite as resedimented detrital particles, advent of non-marine red beds; e.g. Roscoe 1969), loss of sulphur mass-independent isotope fractionation (Farquhar *et al.* 2000), Lomagundi–Jatuli and Shunga C-cycle perturbations (Schidlowski *et al.* 1976; Karhu and Holland 1996; Melezhik *et al.* 1999*a*) and the hypothesised window of Cyanobacteria evolution (e.g. Fischer *et al.* 2016; Sánchez-Baracaldo and Cardona 2020). Of those, the Lomagundi–Jatuli Event (LJE) has become essentially synonymous with tracking the trend of atmospheric oxygenation (e.g. Karhu and Holland 1996; Bekker and Holland 2012; Lyons *et al.* 2014). The LJE is the largest positive carbonate–carbon isotope ($\delta^{13}C_{carb}$) excursion in Earth history, marked by $\delta^{13}C_{carb}$ values between +5 and 10‰ (and higher) in marine carbonate units tens to several hundreds of metres thick that were deposited between *c.* 2.3 and 2.1 Ga (Melezhik *et al.* 2007; Martin *et al.* 2013; Gumsley *et al.* 2017). Two contrasting hypotheses have been championed for the genesis of the LJE. The first is the consensus view, which interprets the LJE as a synchronous and global-scale disturbance of the carbon cycle linked to changes in the oxygenation state of the ocean–atmosphere system such that, following the Great Oxidation Event (Holland 2006; although see Ohmoto 2020 for an alternative perspective), a biogeochemical feedback was established with atmospheric O_2 rising and falling in concert with co-varying fluctuations between oxidative weathering of continental landmasses, nutrient fluxes and primary productivity (Karhu and Holland 1996; Bekker and Holland 2012; Planavsky *et al.* 2012; Canfield *et al.* 2013; Scott *et al.* 2014; Bellefroid *et al.* 2018; Miyazaki *et al.* 2018; Ossa Ossa *et al.* 2018; Hodgskiss *et al.* 2019). The second view is advocated by a minority of workers such as Melezhik *et al.* (1999*b*) and Frauenstein *et al.* (2009) who interpret high C-isotope values of the LJE as due to processes bespoke to palaeoenvironmental settings within individual sedimentary basins (e.g. organic burial rate, sediment flux, evaporation, methanogenesis)

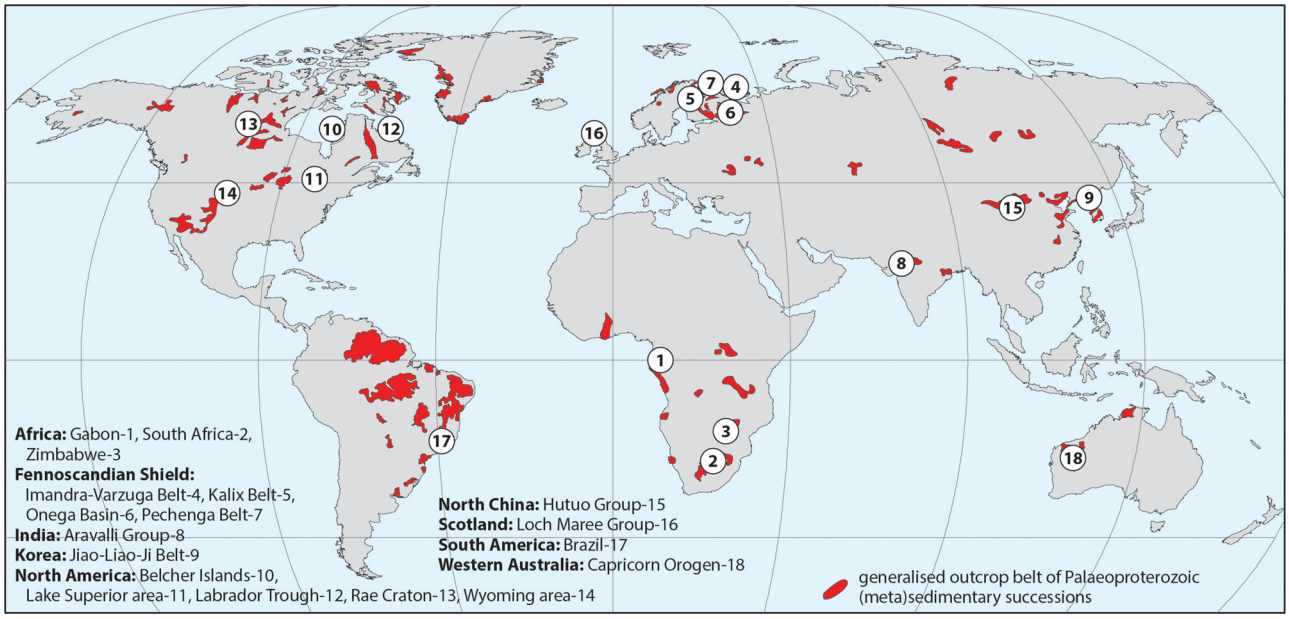

Fig. 1. Generalized map of Paleoproterozoic outcrop belts. Circled numbers indicate those successions utilized in this study. See Supplementary material for data and data sources.

that enhance a plausibly global signal. Central specifically to the consensus view is the conjecture that the highly positive $\delta^{13}C_{carb}$ values of the LJE are representative of the dissolved inorganic carbon (DIC) reservoir of the global ocean which, in turn, underpins the paradigm that the carbon cycle of the LJE and atmospheric oxygenation are directly interrelated (Schidlowski 1988; Karhu and Holland 1996; Planavsky *et al.* 2012; Lyons *et al.* 2014; Daines *et al.* 2017; Bellefroid *et al.* 2018). Here we assess this paradigm by analysing the relationship between carbon isotope data and facies (i.e. palaeoenvironment) for LJE-bearing marine carbonate rocks worldwide (Fig. 1). Because many LJE-bearing successions are lean in organic carbon, our focus is on carbonate–carbon isotope data.

The LJE and the carbon cycle

The connection between key fluxes of carbon as carbonate precipitated out of the marine DIC reservoir and the amount buried as organic matter, including the respective isotopic compositions of each flux, has been commonly evaluated within a framework of mass balance and used in evaluating the pattern and tempo of the global carbon cycle (e.g. Schidlowski 1988; Kump 1991; Hayes and Waldbauer 2006; Mason *et al.* 2017). With few exceptions, the $\delta^{13}C$ value of marine DIC has remained largely within a window of $0 \pm 4‰$ for most of geological time (e.g. Schidlowski 1988; Prokoph *et al.* 2008). The LJE is one of the most remarkable of those exceptions, and hypotheses relying on mass balance have struggled to explain the vast amounts of organic matter that would need to be buried to generate such positive $\delta^{13}C_{carb}$ values (e.g. Karhu and Holland 1996; Aharon 2005; Holland 2006) or have opted to offer speculations invoking an unprecedented spike in primary productivity (e.g. Bekker and Holland 2012). The postulated net outcome of either is an extraordinary pulse in atmospheric oxygen. Other models invoke tectonics driving exhumation and erosion of older sedimentary rocks that, in turn, drive fluctuations in the isotopic composition of the carbon flux entering the marine realm to generate C-isotope excursions in lieu of changes to primary productivity (e.g. Kump 1991; Miyazaki *et al.* 2018), or attribute C-isotope excursions to changing intensities and proportions of chemical versus physical weathering, in part linked to tectonics, such as supercontinent cycles (e.g. Shields and Mills 2017). Our purpose is not to evaluate the veracity of these various models. Rather, our work assesses the key premise that underpins the LJE paradigm, namely, that the magnitude and duration of its $\delta^{13}C_{carb}$ values are an accurate archive of the C-isotopic composition of the global ocean between 2.3 and 2.1 Ga. All concepts and models that use the LJE as evidence of the redox evolution of Earth's surface environments and initial rise and proliferation of free di-oxygen rely on that premise to be true.

Methods

We compiled a database consisting of 14 943 published $\delta^{13}C_{carb}$ data: 11 557 data are for the time interval 3.0–1.0 Ga, which includes 2038

Table 1. *Summary $\delta^{13}C_{carb}$ data for Lomagundi–Jatuli Event successions (N = number of measurements; C.I. = confidence interval). See Supplementary material for data and data sources*

Table 1. Lomagundi–Jatuli Event (LJE) $\delta^{13}C_{carb}$ (‰ V-PDB) summary data

	Palaeoenvironment	N	Bootstrapped mean	Bootstrap mean 95% C.I. lower	Bootstrap mean 95% C.I. upper
Francevillian–Karelia–Kola regions	intertidal–coastal–sabkha (evaporitic)	273	9.3	9.1	9.5
	Nearshore-marine–inner shelf	325	6.8	6.6	6.9
	open and deeper marine	130	2.0	1.6	2.3
all LJE successions worldwide	intertidal–coastal–sabkha (evaporitic)	562	8.1	7.8	8.4
	Nearshore-marine–inner shelf	705	6.2	6.1	6.4
	open and deeper marine	771	1.5	1.3	1.7

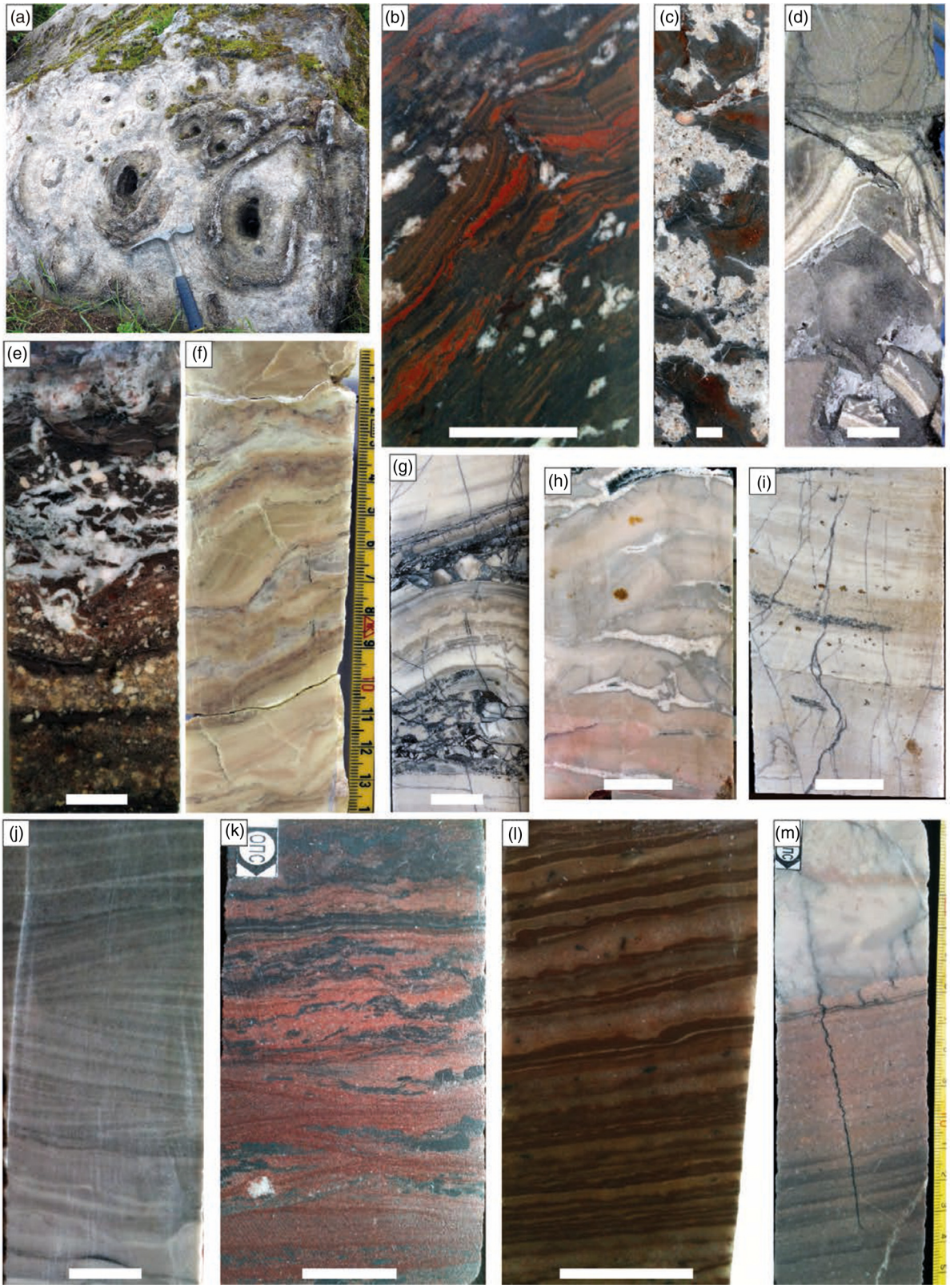

Fig. 2. Coastal–evaporitic–nearshore-marine facies in Lomagundi–Jatuli Event (LJE)-bearing strata of the Onega (a–c, e, f, h, k–m) and Franceville (d, g, i, j) Basins. (**a**) Stromatolites. (**b**) Tepee in red–grey mudstone with evaporite pseudomorphs. (**c**) Evaporite pseudomorph in red–grey mudstone. (**d**). Tepee developed on palaeokarst breccia and eroded by overlying dolostone grainstone. (**e**). Poorly sorted coarse doloarenite and mudstone overlain by disrupted red–brown mudstone with abundant chicken wire fabric. (**f**)–(**h**) Micritic dolostone broken and disrupted by variably developed palaeokarst and evaporite pseudomorph fabrics. (**i**), (**j**) Cross-bedded doloarenite. (**k**) Herringbone cross-lamination with mud drapes. (**l**) Tidal couplets of graded fine doloarenite and red–grey mudstone–dolomarl. (**m**) Tidal bundle of fine doloarenite and grey dolomarl and mudstone with abundant millimetre-scale gypsum pseudomorph needles overlain by dolorudite. Scale bars *c.* 2 cm.

$\delta^{13}C_{carb}$ data from LJE-bearing rocks worldwide. Of the latter, 188 are new $\delta^{13}C_{carb}$ and $\delta^{18}O_{carb}$ isotope data obtained on carbonate rock samples from outcrops of the LJE-bearing Tulomozero Formation in the Onega Basin, NW Russia, at Raiguba (62°22.107′N, 033° 47.129′E) and Shunga (62°36.697′N, 034° 49.457′E) and the portion of the Onega Parametric Hole drill core containing the Tulomozero

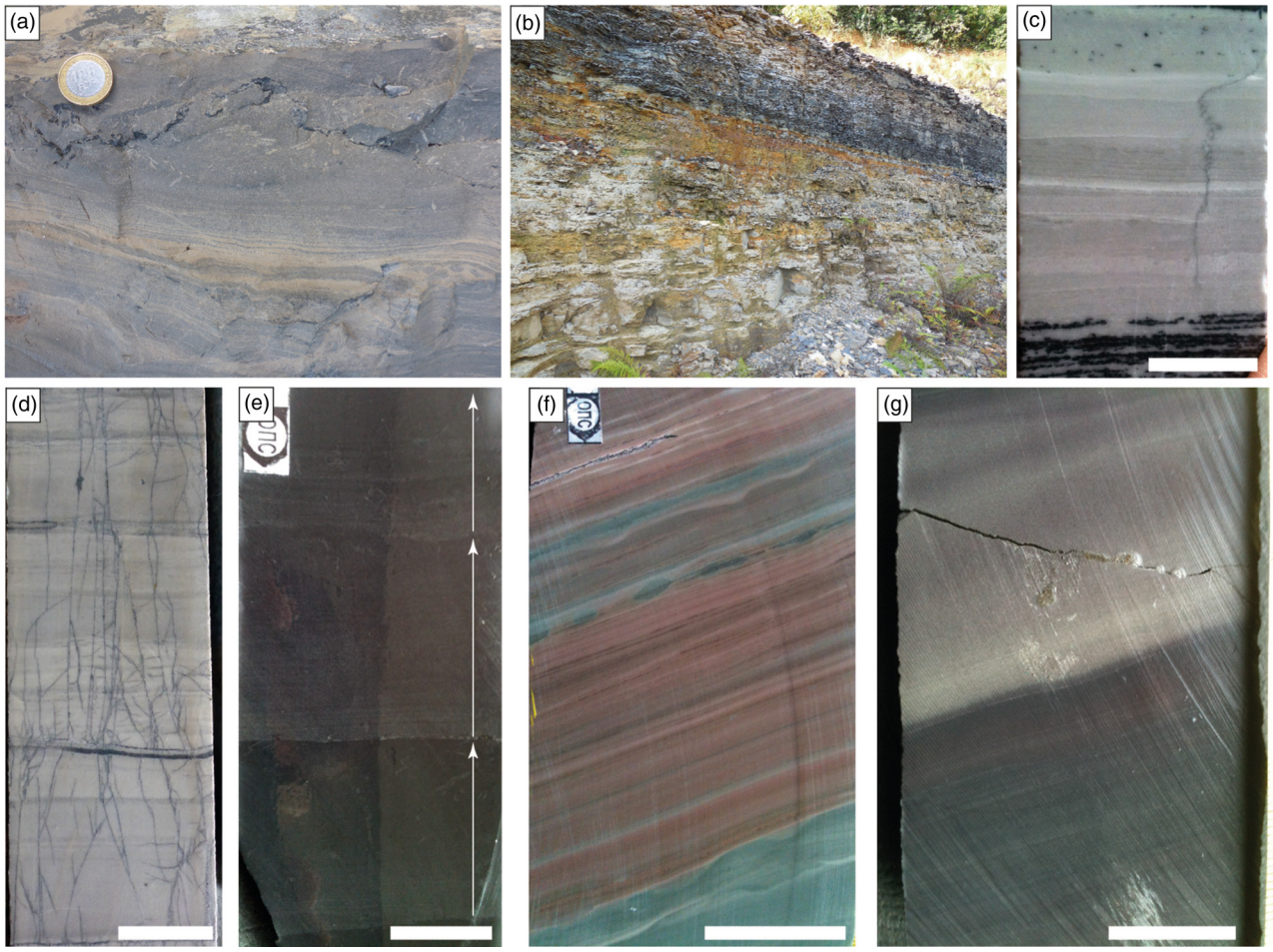

Fig. 3. Open- and deeper-marine facies of LJE-bearing strata in Franceville (a–d) and Onega (e–g) basins. (**a**) Low-angle laminated graded fine doloarenite beds overlain by flake–breccia debrite (coin *c.* 2 cm). (**b**) Dark grey to black shale (outcrop *c.* 5 m in height; contact with dolostone of 3a at base of ledge); pale colours represent deeply weathered intervals. (**c**), (**d**) Thin graded beds of fine dolostone with sets of low-angle plane- to wavy-parallel laminae. (**e**)–(**g**) Grey and cream–pink–green fine dolostone ('krivozerite') in millimetre- to centimetre-thick graded beds marked by millimetre-scale ripples and plane- to wavy-parallel laminae; arrows in 3e denote individual graded beds. Scale bars *c.* 2 cm.

Formation and lower part of the overlying Zaonega Formation. The remaining 3386 data are from Phanerozoic carbonate rocks deposited in environments ranging from sabkha to open ocean and used as a comparator for the LJE. All data and their sources are reported in the Supplementary material. For the new data, measurements were made on a Thermo Scientific Delta V Advantage continuous flow isotope ratio mass-spectrometer in the Department of Geology, University of Tartu, Estonia, following standard protocols. C and O data are reported in per mil (‰) deviation relative to the Vienna PeeDee Belemnite (V-PDB) and standard reproducibility was better than ±0.2‰ at 1σ. In constructing the database of published $\delta^{13}C_{carb}$ values for the 3.0–1.0 Ga rocks, we included only those data that record primary depositional (or nearly so) conditions as per original authors' reporting of petrographic features, C–O isotope cross-plots and key element ratios. We excluded data from rocks that experienced significant post-depositional isotopic resetting and from features of clearly later diagenetic origin (e.g. concretions, cements), as well as carbonate rocks associated with banded-iron formation. Data are evaluated in 100 Myr bins (geons of Hofmann 1990), using the inferred depositional ages reported in the literature.

Sample means were determined by the bootstrap method using an approach described in Keller and Schoene (2012) and Cox *et al.* (2018) which enables estimation of the sampling bias on statistics (mean, median, etc.) whereby a synthetic dataset (bootstrap sample) is created by random independent sampling with replacement from an existing sample (population). The statistics of interest are estimated for each bootstrap sample and each step is repeated numerous times obtaining estimates that can be treated for additional statistical inferences (mean, standard deviation, confidence interval, etc.). The bootstrapped means and confidence intervals reported in Table 1 and Supplementary material were calculated from 10 000 repetitions. The sample bias of the binned data was assessed further by jackknife estimates (Tukey 1958) that were in all cases in agreement with bootstrapped means (jackknife bias = 0). Jackknife procedure is similar to the bootstrap method but sampling is done without replacement and was developed for estimating the variance and bias of large datasets. During the jackknife procedure, a statistic estimate is calculated leaving out one observation at a time from the sample set. Similar to the bootstrap method, the statistic of an estimate for the bias can be calculated from the population of the repeated calculations.

Facies of LJE-bearing successions and C-isotope values

We focus here on two archetypal LJE-bearing successions: the Franceville Basin, Gabon, and the Karelia (Onega Basin)–Kola (Pechenga–Imandra Varzuga Belts) regions, Russia. These have been studied extensively by many workers including ourselves, the former by Préat *et al.* (2011), Canfield *et al.* (2013), Ossa Ossa *et al.* (2018) and Bakakas Mayika *et al.* (2020) and the latter by Galimov *et al.* (1968), Yudovich *et al.* (1990). Akhmedov *et al.* (1993), Karhu (1993) and Tikhomirova and Makarikhin (1993) and via the International

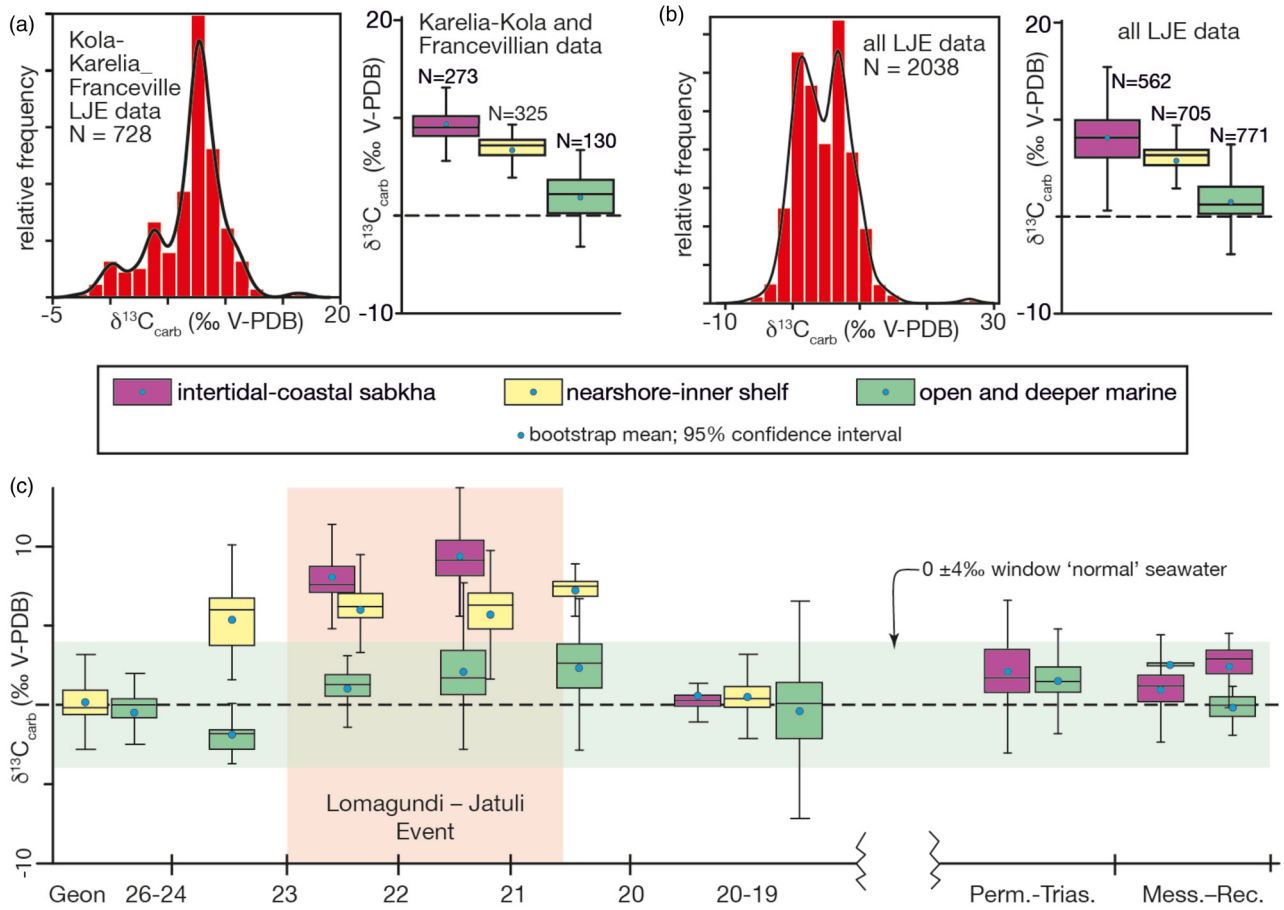

Fig. 4. Box-and-whisker plots for $\delta^{13}C_{carb}$ data classified by palaeoenvironmental setting. (**a**) Data for the Francevillian and Karelia–Kola regions. (**b**) LJE data worldwide. (**c**) Timeline trend of palaeoenvironmental settings from Neoarchaean through to specific Phanerozoic time periods (Rec, Recent; Mess, Messinian; Perm, Permian; Trias, Triassic). See Supplementary material for C-isotope data.

Continental Scientific Drilling Program's Fennoscandia–Arctic Russia Deep Early Earth Project (FAR-DEEP; Melezhik *et al.* 2013*a*). Because exposure is poor in both regions, building sedimentological and stratigraphic frameworks relies on drill core to supplement outcrop-based observations. As examples, we highlight the Onega Parametric Hole and FAR-DEEP cores in the Onega Basin and LST12 core from the Lastoursville area of the Franceville Basin. These cores are representative of the sedimentology and stratigraphy common to LJE-bearing successions in those regions and, incidentally, to many other LJE-bearing localities elsewhere.

In both the Franceville and Onega Basins the LJE-bearing successions begin with interbedded pale grey to pink dolostone and red–brown–grey mudstone and dolomarl containing variable proportions of shallow-water sedimentary structures including stromatolites, evaporite fabrics and (palaeo)karst, tidal couplets and cross-bedded grainstones, and ripple and herring-bone cross-lamination replete with reactivation surfaces and mud drapes (Fig. 2). These facies occur in units many tens to several hundreds of metres thick and pass upward into very fine dolostone, dolomarl, mudstone and shale in units many tens of metres thick marked by sets of planar- to wavy-parallel laminae with small ripples, in places hummocky cross-stratification, and millimetre- to centimetre-thick graded beds and rhythmite (Fig. 3); colours vary from grey to black excepting one 10–30 m thick unit in the Onega Basin that is cream–pink–green in colour (more on this unit below). The vertical facies successions in both basins offer clear sedimentological evidence for a transition from nearshore-marine–intertidal and in places coastal sabkha settings for the pink–grey dolostone interval into open and deeper marine settings (i.e. depths near or below storm-wave base) for the overlying fine dolostone–dolomarl–mudstone interval. This interpretation is in general agreement with all previous workers (e.g. Brasier *et al.* 2011; Préat *et al.* 2011; Melezhik *et al.* 2013*b*; Ossa Ossa *et al.* 2018; Bakakas Mayika *et al.* 2020) and permits us to recognize three main palaeoenvironmental clusters: intertidal and in places sabkha settings, nearshore-marine–inner shelf settings, and open and deeper marine settings.

The LJE-bearing successions in the Franceville Basin and Karelia–Kola regions share another trait; they display an overall declining stratigraphic trend in $\delta^{13}C_{carb}$ values from *c.* +6–10‰ in the coastal–nearshore-marine intervals to 0–5‰ in the overlying open- and deeper-marine intervals. In the consensus model, this trend is interpreted as recording the termination of the LJE (e.g. Melezhik *et al.* 2007; Canfield *et al.* 2013; Ossa Ossa *et al.* 2018). A salient observation, though, is that this trend coincides with facies changes such that C-isotope values correlate directly with palaeoenvironment (Table 1; Fig. 4a): the mean value for coastal intertidal–sabkha facies is +9.3 ± 1.7‰, for nearshore marine–inner shelf facies it is +6.8 ± 1.5‰ and for open- and deeper-marine facies it is +2.0 ± 2.1‰. Thus, the high $\delta^{13}C_{carb}$ values that define the LJE in the Karelia–Kola and Francevillian successions are an expression of facies; they are present in nearshore-marine–coastal–sabkha settings but minor in open- and deeper-marine settings. The question that arises is: is it merely a coincidence that facies changes and the trend of $\delta^{13}C_{carb}$ values are synchronized in those regions?

Assessing the LJE globally

Golovkinsky–Walther's Law is a fundamental guiding principle in stratigraphy. First articulated in the mid-1800s by Nikolai

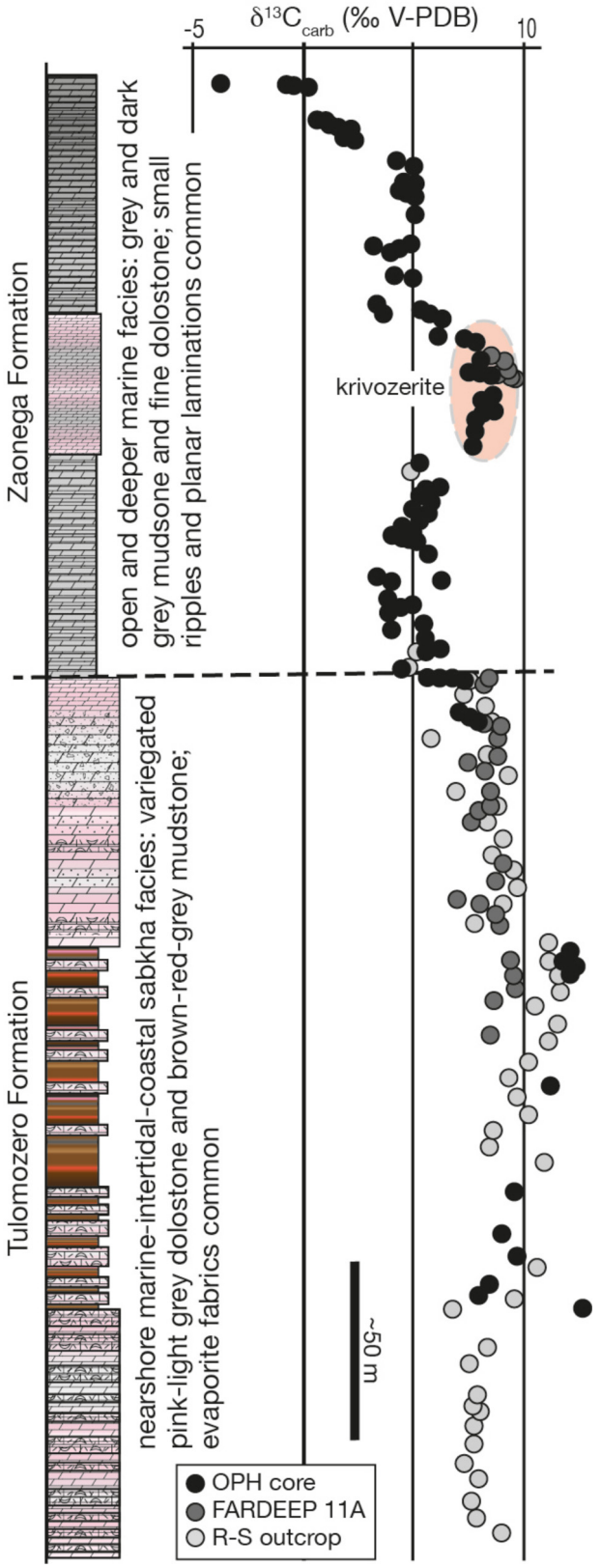

Fig. 5. C-isotope profile of Tulomozero and lower part of Zaonega Formations, Onega Basin. OPH, Onega Parametric Hole; R-S, Raiguba and Shunga localities. See Supplementary material for C-isotope data.

Golovkinsky working in the Perm district of Russia (Nurgalieva *et al.* 2007) and later independently by Johannes Walther working in the Austrian Alps (Walther 1894), it states that in a vertical succession of strata unbroken by significant hiatal surfaces, rocks layered one on top of the other were deposited in coeval, laterally adjacent environments. Given that C-isotope values and facies changes co-vary in the Francevillian and Karelia–Kola LJE-bearing successions, it is important to assess if the trend in $\delta^{13}C_{carb}$ in those successions can be attributed to original environmental isotopic gradients now superposed stratigraphically, as per Golovkinsky–Walther's Law, rather than recording global ocean DIC as per the consensus view.

To determine this, we expanded our analysis to encompass published data for LJE-bearing rocks worldwide and focused on studies in which authors provided sufficient sedimentological details to enable assigning their facies interpretations and $\delta^{13}C_{carb}$ data into our palaeoenvironmental categories of intertidal–coastal–sabkha, nearshore marine–inner shelf, and open- and deeper-marine. Strikingly, even though $\delta^{13}C_{carb}$ values in the worldwide dataset range between *c.* −10‰ and *c.* +26‰, for the entire 200–300 million year duration of the LJE there is a strong co-dependence between facies changes and $\delta^{13}C_{carb}$ values (Table 1, Fig. 4b): the mean value for the open-marine realm was +1.5 ± 2.4‰, for the nearshore-marine–inner shelf +6.2 ± 2.0‰ and for intertidal–sabkha settings +8.1 ± 3.8‰. To place the LJE in context, we extended our analyses further to include marine carbonate rocks from 3.0 to 1.0 Ga, and also from times of major Phanerozoic evaporite deposits (Permo-Triassic, Messinian, modern sabkhas), given that LJE-bearing successions can contain variable amounts of evaporite pseudomorphs. This analysis shows that $\delta^{13}C_{carb}$ values of open- and deeper-marine carbonate rocks for all assessed time periods, *including* LJE-bearing successions, were consistently within 0 ± 4‰ and comparable to that for the modern open ocean DIC reservoir (Fig. 4c). The data confirm that the uniquely highly positive $\delta^{13}C_{carb}$ values of the LJE are themselves facies dependent, found dominantly in nearshore-marine and coastal settings and mostly absent in open- and deeper-marine settings. Hence, these highly positive $\delta^{13}C_{carb}$ values are not representative of either the global DIC pool or the operation of the global carbon cycle.

The significance of high C-isotope values occurring in deeper-water facies

In a few LJE-bearing successions (e.g. Tulomozero–Zaonega Formation; Silverton Formation, South Africa; Frauenstein *et al.* 2009) high $\delta^{13}C_{carb}$ values are known for rocks interpreted as recording more open- and deeper-marine settings. We have first-hand knowledge of one of those and offer it as both an exemplar and explanation for such occurrences (see Fig. 5). In the Onega Basin, the upper part of the LJE-bearing Tulomozero Formation consists of sabkha and shallow-marine evaporite–fabric-bearing dolostone and mudstone (Brasier *et al.* 2011; Melezhik *et al.* 2013*b*) with $\delta^{13}C_{carb}$ between +6 and 12‰. Above these rocks is a several tens-of-metres thick unit consisting of centimetre- to decimetre-thick beds of grey to dark grey dolostone–dolomarl–mudstone with $\delta^{13}C_{carb}$ from +3 to 5‰, overlain by cream–pink–green fine dolostone–dolomarl marked by $\delta^{13}C_{carb}$ between +6 and 9‰ (these dolostones are termed *krivozerite* by Russian workers) and then a return to grey–dark grey dolostone–dolomarl–mudstone in which $\delta^{13}C_{carb}$ declines to 0‰. This interval passes upward into organic-rich and pyritiferous deep-marine mudstones of the Zaonega Formation (e.g. Črne *et al.* 2013, 2014; Kreistmann *et al.* 2019; Paiste *et al.* 2020).

Assessed within the construct of conventional thinking about the LJE, such a fluctuating C-isotope pattern is taken as evidence of oscillating productivity–oxygenation episodes (e.g. Bekker and Holland 2012). However, there is a more likely, albeit less grand, explanation. Detailed petrography, mineralogy and sedimentology by Črne *et al.* (2014) showed that many carbonate beds in the lower part of the Zaonega Formation were resedimented (e.g. Fig. 3e), emplaced by turbidity currents inferred to have originated from laterally adjacent shallower settings of the Tulomozero Formation. Such an interpretation is consistent with evidence for erosion and transport of carbonate detritus as per the abundance of cross-bedded doloarenite

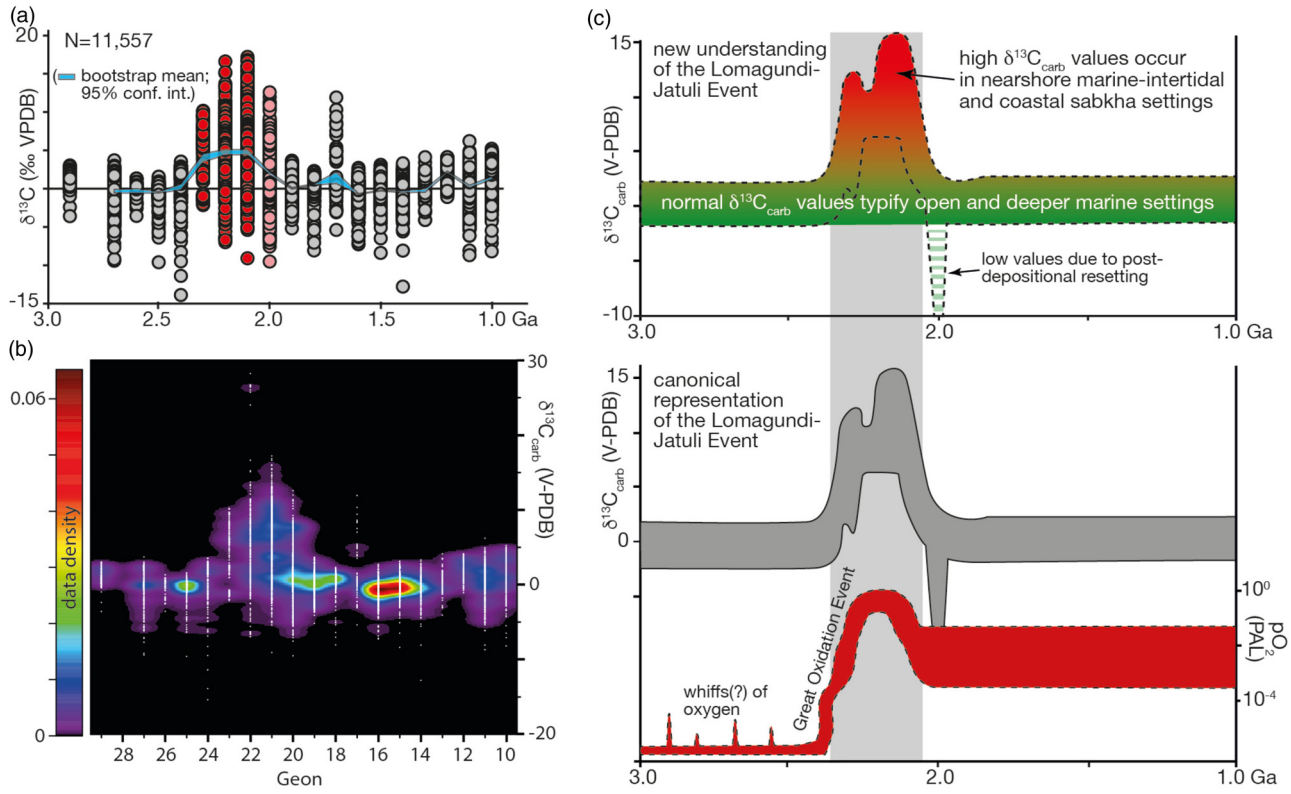

Fig. 6. $\delta^{13}C_{carb}$ data for marine carbonate rocks between 3.0 and 1.0 Ga in age in 100 Myr age bins (see Supplementary material for sources of data). (**a**) LJE-bearing successions are in red and those recording the purported decline of the LJE in light red; running bootstrap average shown as a blue line. (**b**) 2D density plot that shows the abundance and consistency of $\delta^{13}C_{carb}$ values between 0 and 4‰ across the entire 2 Gyr time span. (**c**). The lower panel shows the consensus view of a direct one-to-one match between the LJE and postulated rise in atmospheric pO_2 (PAL: present atmospheric level; adapted after Lyons *et al.* 2014). The upper panel shows the new understanding of the LJE excursion as a consequence of palaeoenvironmental setting (consensus view is shown by dashed outline). The light-grey bar highlights the LJE. Deeply negative $\delta^{13}C_{carb}$ values that post-date the LJE have been shown in two studies of the Onega Basin rocks to reflect post-depositional overprinting or methane recycling (Črne *et al.* 2014; Kreistmann *et al.* 2019, 2020).

and dolorudite in the Tulomozero rocks (e.g. Fig. 2i). Applying Occam's razor, the episodic return of high $\delta^{13}C_{carb}$ values in the deeper-water lower Zaonega Formation represents sediment derived from the ^{13}C-rich shallow-water Tulomozero Formation intermixed with carbonate of the open- and deeper-marine DIC pool with its 'normal' C-isotopic composition. We propose that other postulated open- and deeper-marine units with very positive $\delta^{13}C_{carb}$ values (e.g. Silverton Formation) may also reflect redeposition of ^{13}C-rich carbonate transported from adjacent shallower environments.

The LJE: a new understanding

Our analyses reveal that the highest-amplitude, longest-lived deviation from what is considered to be 'normal' C-cycle functioning over the past four billion years is tied directly to facies changes. Everywhere during the 200–300 million year duration of the LJE, the C-isotopic composition of facies recording open- and deeper-marine conditions remained 'normal' whereas those deposited in nearshore–coastal realms sustained ^{13}C-enriched isotopic compositions. Thus, the canonical image of the LJE as a high-amplitude C-isotope bulge punctuating an otherwise undisturbed *c.* two billion year continuum of relatively normal marine C-isotope values is misleading (Fig. 6). Instead, our findings show that the C-isotope pattern of the LJE is a record of *contemporaneous* lateral gradients in the isotopic composition of DIC pools, ranging from normal open-marine values of *c.* 0‰ $\delta^{13}C_{carb}$ to extremely high values of +16‰ and even higher, in nearshore-marine–coastal settings. Stated simply, trends of C-isotope profiles in LJE-bearing successions are a consequence of Golovkinsky–Walther's Law, i.e. strata superposed during sedimentation occurring concurrently during lateral migration of coeval depositional environments characterized by distinct local DIC pools.

We thus conclude that the $\delta^{13}C_{carb}$ trends do not record a global-scale perturbation of the carbon cycle, nor can they be used to infer a worldwide C-isotopic composition of marine DIC. In these aspects, the LJE is not a singularity in that the link between facies changes and positive $\delta^{13}C_{carb}$ excursions marked by sustained values of +5–10‰ and locally higher for stratigraphically significant intervals is known from other times in Earth history. Studies combining careful sedimentology and petrography with isotope geochemistry show that co-variation between facies and $\delta^{13}C_{carb}$ values is common and can modify global signals; examples include the Cryogenian Tayshir Member of the Tsagaan Oloom Formation in Mongolia (Macdonald *et al.* 2009; Bold *et al.* 2016) and Etina Formation in Australia (Rose *et al.* 2012), Ediacaran Hüttenberg Formation in Namibia (Cui *et al.* 2018), end-Ordovician Hirnantian strata (Jones *et al.* 2020) and Silurian Ireviken and Lau Events in the Baltic Basin (Wigforss-Lange 1999; Rose *et al.* 2019). Studies of C-isotope process-response in recent and modern depositional environments provide additional credence to our scenario that the LJE is a record of lateral isotopic gradients of contemporaneous DIC pools. Those studies show shallow-marine settings may have 2–5‰ or more variability in $\delta^{13}C_{carb}$ relative to that of the open ocean (e.g. Swart 2008; Geyman and Maloof 2019). These findings are apropos to the LJE, consistent with and substantiating interconnectedness between facies changes and $\delta^{13}C_{carb}$ values. It is worth noting that, although exceptionally high $\delta^{13}C_{carb}$ values (>15‰) are known for some LJE-bearing strata, the number of such values total 24 out of the 2038 values we amassed (i.e., *c.* 1% of the data) making them more a curiosity than a norm, much like modern environments where carbonates form with $\delta^{13}C_{carb}$ in excess of +15‰ (e.g. Birgel *et al.* 2015).

Neither the modern nor ancient examples, though, explain why nearshore-marine and coastal settings during the LJE reached such

high enrichments in ^{13}C. For this, we do not yet have an answer and at this time prefer not to offer speculative scenarios. We highlight, however, that many LJE-bearing successions are shallow-marine carbonate rocks associated with evaporitic and sabkha-like features. Evaporation pond brines are known to have $\delta^{13}C$ values of +8–16‰ and brine-evaporation experiments have generated values of +16–35‰ (Stiller *et al.* 1985), that overlap those of the LJE. Thus, modern and ancient examples hint of the possibility of a yet undetermined process-response link between C-isotope composition, evaporation and microbial ecosystems to create conditions for widespread ^{13}C-enrichment in shallow-marine environments during mid-Paleoproterozoic time.

The LJE and Earth's oxygenation: summary and conclusions

Our analysis integrating 14 943 $\delta^{13}C_{carb}$ measurements with sedimentology for marine carbonate rocks 3.0–1.0 Ga in age and, including appropriate Phanerozoic deposits, reveals that ^{13}C enrichment during the 200–300 Myr span of the LJE was restricted to specific environments: $\delta^{13}C_{carb}$ values from nearshore-marine and coastal–sabkha settings yield means of 6.2 ± 2.0‰ and 8.1 ± 3.8‰, respectively. In contrast, carbonate sediments deposited in open- and deeper-marine settings are marked by $\delta^{13}C_{carb}$ values averaging 1.5 ± 2.4‰, consistent with the mean C-isotope composition of oceans throughout most of geological time. These results indicate that high $\delta^{13}C_{carb}$ values, the hallmark feature of the LJE, archive locally heterogeneous C-isotopic composition of *contemporaneous* DIC pools of *coeval* depositional settings. Our findings necessitate rethinking of models that rely on the LJE as a proxy for the global carbon cycle and atmospheric oxygen levels and highlight an unresolved question: why, during the middle part of the Paleoproterozoic Era, did coastal–nearshore-marine and evaporite settings acquire such high ^{13}C-enriched values?

Acknowledgments We thank the Institute of Geology, Karelian Research Centre of the Russian Academy of Sciences, Petrozavodsk, Russia, and the Department of Geology, Université des Sciences et Techniques de Masuku, Franceville, Gabon, for their hospitality and help in accessing drill cores and outcrops. We thank E. Stüeken and J. Raven for insightful comments that improved earlier versions of this manuscript, and D. Fike and A. Brasier for reviews. We also thank G. Shields for providing raw data compiled originally for Shields and Vezier (2002).

Author contributions **ARP**: conceptualization (equal), investigation (equal), writing – original draft (equal), writing – review & editing (equal); **KK**: conceptualization (equal), investigation (equal), writing – original draft (equal), writing – review & editing (equal); **AL**: conceptualization (equal), investigation (equal), writing – original draft (equal), writing – review & editing (equal); **AEF**: conceptualization (equal), writing – original draft (equal), writing – review & editing (equal); **TK**: conceptualization (equal), investigation (equal), writing – original draft (equal), writing – review & editing (equal); **YED**: conceptualization (equal), investigation (equal); **AER**: conceptualization (equal), investigation (equal); **DVR**: conceptualization (equal), investigation (equal); **PVM**: conceptualization (equal), investigation (equal), writing – original draft (equal); **MM**: conceptualization (equal), investigation (equal); **KB**: conceptualization (equal), investigation (equal); **MSWH**: writing – original draft (equal), writing – review & editing (equal)

Funding K.K., A.L. and T.K. received funding from Estonian Science Agency Project PRG447 and Yu.D., A.R., D.R. and P.M. were supported by the state assignment of the Institute of Geology, Karelian Research Centre of the Russian Academy of Sciences.

Data availability The datasets generated during and/or analysed during the current study are available in the Supplementary material included with this manuscript.

Scientific editing by Heda Agic

References

Aharon, P. 2005. Redox stratification and anoxia of the early Precambrian oceans: implications for carbon isotope excursions and oxidation events. *Precambrian Research*, **137**, 207–222, https://doi.org/10.1016/j.precamres.2005.03.008

Akhmedov, A.M., Krupenik, V.A., Makarikhin, V.V. and Medvedev, P.V. 1993. *Carbon Isotope Composition of Carbonates in the Early Proterozoic Sedimentary Basins*. Printed report, Institute of Geology of the Karelian Scientific Centre, Petrozavodsk [in Russian].

Bakakas Mayika, K., Moussavou, M., Prave, A.R., Lepland, A., Mbina, M. and Kirsimäe, K. 2020. Paleoproterozoic Francevillian succession of Gabon and the Lomagundi-Jatuli Event. *Geology*, **48**, 1099–1104, https://doi.org/10.1130/G47651.1

Bekker, A. and Holland, H.D. 2012. Oxygen overshoot and recovery during the early Paleoproterozoic. *Earth and Planetary Science Letters*, **317–318**, 295–304, https://doi.org/10.1016/j.epsl.2011.12.012

Bellefroid, E.J., Hood, A.v.S., Hoffman, P.F., Thomas, M.D., Reinhard, C.T. and Planavsky, N.J. 2018. Constraints on Paleoproterozoic oxygen levels. *Proceedings of the National Academy of Sciences U.S.A.*, **115**, 8104–8109, https://doi.org/10.1073/pnas.1806216115

Birgel, D., Meister, P. *et al.* 2015. Methanogenesis produces strong ^{13}C enrichment in stromatolites of Lagoa Salgada, Brazil: a modern analogue for Palaeo-/Neoproterozoic stromatolites? *Geobiology*, **13**, 245–266, https://doi.org/10.1111/gbi.12130

Bold, U., Smith, E.F. *et al.* 2016. Neoproterozoic stratigraphy of the Zavkhan terrane of Mongolia: the backbone for Cryogenian and early Ediacaran chemostratigraphic records. *American Journal of Science*, **316**, 1–63, https://doi.org/10.2475/01.2016.01

Brasier, A.T., Fallick, A.E., Prave, A.R., Melezhik, V.A. and Lepland, A. and FAR-DEEP Scientists 2011. Coastal sabkha dolomites and calcitised sulphates preserving the Lomagundi-Jatuli carbon isotope signal. *Precambrian Research*, **189**, 193–211, https://doi.org/10.1016/j.precamres.2011.05.011

Canfield, D.E., Ngombi-Pemba, L. *et al.* 2013. Oxygen dynamics in the aftermath of the Great Oxidation of Earth's atmosphere. *Proceedings of the National Academy of Sciences U.S.A.*, **110**, 16736–16741, https://doi.org/10.1073/pnas.1315570110

Cox, G.M., Lyons, T.W., Mitchell, R.N., Hasterok, D. and Gard, M. 2018. Linking the rise of atmospheric oxygen to growth in the continental phosphorus inventory. *Earth and Planetary Science Letters*, **489**, 28–36, https://doi.org/10.1016/j.epsl.2018.02.016

Črne, A.E., Melezhik, V.A. *et al.* 2013. Zaonega formation: FAR-DEEP Holes 12A-12B, and neighbouring quarries. *In*: Melezhik, V.A. *et al.* (eds) *Reading the Archive of Earth's Oxygenation*, **2**. Springer, Berlin, 946–1007.

Črne, A.E., Melezhik, V.A., Lepland, A., Fallick, A.E., Prave, A.R. and Brasier, A.T. 2014. Petrography and geochemistry of carbonate rocks of the Paleoproterozoic Zaonega Formation, Russia: documentation of ^{13}C–depleted non-primary calcite. *Precambrian Research*, **240**, 79–93, https://doi.org/10.1016/j.precamres.2013.10.005

Cui, H., Kaufman, A., Peng, Y., Liu, X.-M., Plummer, R. and Lee, E. 2018. The Neoproterozoic Hüttenberg 13C anomaly: genesis and global implications. *Precambrian Research*, **313**, 242–262, https://doi.org/10.1016/j.precamres.2018.05.024

Daines, S.J., Mills, B.J.W. and Lenton, T.M. 2017. Atmospheric oxygen regulation at low Proterozoic levels by incomplete oxidative weathering of sedimentary organic carbon. *Nature Communications*, **8**, 14379, https://doi.org/10.1038/ncomms14379

Farquhar, J., Bao, H. and Thiemens, M. 2000. Atmospheric influence of Earth's earliest sulfur cycle. *Science*, **289**, 756–758, https://doi.org/10.1126/science.289.5480.756

Fischer, W.W., Hemp, J. and Johnson, J.E. 2016. Evolution of oxygenic photosynthesis. *Annual Reviews of Earth Planetary Science*, **44**, 647–683, https://doi.org/10.1146/annurev-earth-060313-054810

Frauenstein, F., Veizer, J., Beukas, N., Van Niekerk, H.S. and Coutzee, L.L. 2009. Transvaal Supergroup carbonates: implications for Paleoproterozoic $\delta^{18}O$ and $\delta^{13}C$ records. *Precambrian Research*, **175**, 149–160, https://doi.org/10.1016/j.precamres.2009.09.005

Galimov, E.M., Kuznetsova, N.G. and Prokhorov, V.S. 1968. On the problem of the Earth's ancient atmosphere composition in connection with results of isotope analysis of carbon from the Precambrian carbonates. *Geochemistry*, **11**, 1376–1381.

Geyman, E.C. and Maloof, A.C. 2019. A diurnal carbon engine explains ^{13}C-enriched carbonates without increasing the global production of oxygen. *Proceedings of the National Academy of Science U.S.A.*, **116**, 24433–24439, https://doi.org/10.1073/pnas.1908783116

Gumsley, A.P., Chamberlain, K.R., Bleeker, W., Söderlund, U., de Kock, M.O., Larsson, E.R. and Bekker, A. 2017. Timing and tempo of the great oxidation event. *Proceedings of the National Academy of Science U.S.A.*, **114**, 1811–1816, https://doi.org/10.1073/pnas.1608824114

Hayes, J.M. and Waldbauer, J.R. 2006. The carbon cycle and associated redox processes through time. *Philosophical Transactions Royal Society of London B*, **361**, 931–950, https://doi.org/10.1098/rstb.2006.1840

Hodgskiss, M.S.W., Crockford, P.W., Peng, Y., Wing, B.A. and Horner, T.J. 2019. A productivity collapse to end Earth's Great Oxidation. *Proceedings National Academy of Science U.S.A.*, **116**, 17207–17212, https://doi.org/10.1073/pnas.1900325116

Hofmann, H.J. 1990. Precambrian time units and nomenclature—the geon concept. *Geology*, **18**, 340–341, https://doi.org/10.1130/0091-7613(1990)018<0340:PTUANT>2.3.CO;2

Holland, H.D. 2006. The oxygenation of the atmosphere and oceans. *Philosophical Transactions Royal Society of London B*, **361**, 903–915, https://doi.org/10.1098/rstb.2006.1838

Jones, D.S., Brothers, R.W., Crüger Ahm, A-S., Slater, N., Higgins, J.A. and Fike, D.A. 2020. Sea level, carbonate mineralogy, and early diagenesis controlled $\delta^{13}C$ records in Upper Ordovician carbonates. *Geology*, **48**, 194–199, https://doi.org/10.1130/G46861.1

Karhu, J. 1993. *Paleoproterozoic Evolution of the Carbon Isotope Ratios of Sedimentary Carbonates in the Fennoscandian Shield. Geological Survey of Finland Bull*, **371**.

Karhu, J. and Holland, H.D. 1996. Carbon isotopes and rise of atmospheric oxygen. *Geology*, **24**, 876–879, https://doi.org/10.1130/0091-7613(1996)024<0867:CIATRO>2.3.CO;2

Keller, C.B. and Schoene, B. 2012. Statistical geochemistry reveals disruption in secular lithospheric evolution about 2.5 Gyr ago. *Nature*, **485**, 490–493, https://doi.org/10.1038/nature11024

Kreistmann, T., Külaviir, M. *et al.* 2019. Hydrothermal dedolomitisation of carbonate rocks of the Paleoproterozoic Zaonega Formation, NW Russia — Implications for the preservation of primary C isotope signals. *Chemical Geology*, **512**, 43–57, https://doi.org/10.1016/j.chemgeo.2019.03.002

Kreistmann, T., Lepland, A. *et al.* 2020. Oxygenated conditions in the aftermath of the Lomagundi-Jatuli Event: the carbon isotope and rare earth element signatures of the Paleoproterozoic Zaonega Formation, Russia. *Precambrian Research*, **37**, 10585, https://doi.org/10.1016/j.precamres.2020.105855

Kump, L.R. 1991. Interpreting carbon-isotope excursions: Strangelove oceans. *Geology*, **19**, 299–302, https://doi.org/10.1130/0091-7613(1991)019<0299:ICIESO>2.3.CO;2

Lyons, T.W., Reinhard, C.T. and Planavsky, N.J. 2014. The rise of oxygen in Earth's early ocean and atmosphere. *Nature*, **506**, 307–315, https://doi.org/10.1038/nature13068

Macdonald, F.A., Jones, D.S. and Schrag, D.P. 2009. Stratigraphic and tectonic implications of a newly discovered glacial diamictite-cap carbonate couplet in southwestern Mongolia. *Geology*, **37**, 123–126, https://doi.org/10.1130/G24797A.1

Martin, A.P., Condon, D.J., Prave, A.R. and Lepland, A. 2013. A review of temporal constraints for the Palaeoproterozoic large, positive carbonate carbon isotope excursion (the Lomagundi-Jatuli Event). *Earth Science Reviews*, **127**, 242–261, https://doi.org/10.1016/j.earscirev.2013.10.006

Mason, E., Edmonds, M. and Turchyn, A.V. 2017 Remobilization of crustal carbon may dominate volcanic arc emissions. *Science*, **357**, 290–294, https://doi.org/10.1126/science.aan5049

Melezhik, V.A., Fallick, A.E., Filippov, M.M. and Larsen, O. 1999*a*. Karelian shungite—an indication of 2.0-Ga-old metamorphosed oil-shale and generation of petroleum: geology, lithology and geochemistry. *Earth-Science Reviews*, **47**, 1–40, https://doi.org/10.1016/S0012-8252(99)00027-6

Melezhik, V.M., Fallick, A.E., Medvedev, P.V. and Maharikhin, V.V. 1999*b*. Extreme $\delta^{13}C$ enrichment in *c.* 2.0 Ga magnesite-stromatolite-dolomite-'red beds' association in a global context: a case for the world-wide signal enhanced by a local environment. *Earth Science Reviews*, **48**, 71–120, https://doi.org/10.1016/S0012-8252(99)00044-6

Melezhik, V.A., Huhma, H., Condon, D.J., Fallick, A.E. and Whitehouse, M.J. 2007. Temporal constraints on the Paleoproterozoic Lomagundi-Jatuli carbon isotopic event. *Geology*, **35**, 655–658, https://doi.org/10.1130/G23764A.1

Melezhik, V.A., Prave, A.R., Fallick, A.E, Hanski, E.J., Lepland, A., Kump, L.R. and Strauss, H. 2013*a*. *Reading the Archive of Earth's Oxygenation*, **2**. Springer, Berlin.

Melezhik, V.A., Prave, A.R. *et al.* 2013*b*. Tulomozero formation: FAR-DEEP Holes 10A-10B. *In*: Melezhik, V.A. *et al.* (eds) *Reading the Archive of Earth's Oxygenation*, **2**. Springer, Berlin, 773–888.

Miyazaki, Y., Planavsky, N.J., Bolton, E.W. and Reinhard, C.T. 2018. Making sense of massive carbon isotope excursions with an inverse carbon cycle model. *Journal of Geophysical Research. Biogeosciences*, **123**, 2485-2496, https://doi.org/10.1029/2018JG004416

Nurgalieva, N.G., Vinokurov, V.M. and Nurgaliev, D.K. 2007. The Golovkinsky strata formation model, basic facies law and sequence stratigraphy concept: historical sources and relations. *Russian Journal Earth Sciences*, **9**, 1–7.

Ohmoto, H. 2020. A seawatersulfate origin for Earth's volcanic sulfur. *Nature Geoscience*, **13**, 576–583, https://doi.org/10.1038/s41561-020-0601-6

Ossa Ossa, F., Eickmann, B., Hofmann, A., Planavsky, N.J., Asael, D., Pambo, F. and Bekker, A. 2018. Two-step deoxygenation at the end of the Paleoproterozoic Lomagundi Event. *Earth and Planetary Science Letters*, **486**, 70–83, https://doi.org/10.1016/j.epsl.2018.01.009

Paiste, K., Pellerin, A., Zerkle, A.Z., Kirsimäe, K., Prave, A.R., Romashkin, A.E. and Lepland, A. 2020. The pyrite multiple sulfur isotope record of the 1.98 Ga Zaonega Formation: evidence for biogeochemical sulfur cycling in a semi-restricted basin. *Earth and Planetary Science Letters*, **534**, 116092, https://doi.org/10.1016/j.epsl.2020.116092

Planavsky, N.J., Bekker, A., Hofmann, A., Owens, J.D. and Lyons, T.W. 2012. Sulfur record of rising and falling marine oxygen and sulfate levels during the Lomagundi event. *Proceedings National Academy of Sciences U.S.A.*, **109**, 18300–18305, https://doi.org/10.1073/pnas.1120387109

Préat, A., Bouton, P., Thieblemont, D., Prian, J.P., Ndounze, S.S. and Delpomdor, F. 2011. Paleoproterozoic high $\delta^{13}C$ dolomites from the Lastoursville and Franceville basins (SE Gabon): stratigraphic and synsedimentary subsidence implications. *Precambrian Research*, **189**, 212–228, https://doi.org/10.1016/j.precamres.2011.05.013

Prokoph, A., Shields, G.A. and Veizer, J. 2008. Compilation and time-series analysis of a marine carbonate $\delta^{18}O$, $\delta^{13}C$, $^{87}Sr/^{86}Sr$ and $\delta^{34}S$ database through Earth history. *Earth Science Reviews*, **87**, 113–133, https://doi.org/10.1016/j.earscirev.2007.12.003

Roscoe S.M. 1969. *Huronian Rocks and Uraniferous Conglomerates in the Canadian Shield*. *Geological Survey of Canada*, paper 68–40.

Rose, C.V., Swanson-Hysell, N.L., Husson, J.M., Poppick, L.N., Cottle, J.M., Schoene, B. and Maloof, A.C. 2012. Constraints on the origin and relative timing of the Trezona $\delta^{13}C$ anomaly below the end-Cryogenian glaciation. *Earth and Planetary Science Letters*, **319–320**, 241–250, https://doi.org/10.1016/j.epsl.2011.12.027

Rose, C.V., Fischer, W.W., Finnegan, S. and Fike, D.A. 2019. Records of carbon and sulfur cycling during the Silurian Ireviken Event in Gotland, Sweden. *Geochimica et Cosmochimica Acta*, **246**, 299–316, https://doi.org/10.1016/j.gca.2018.11.030

Sánchez-Baracaldo, P. and Cardona, T. 2020. On the origin of oxygenic photosynthesis and Cyanobacteria. *New Phytologist*, **225**, 1440–1446, https://doi.org/10.1111/nph.16249

Schidlowski, M. 1988. A 3800-million-year isotopic record of life from carbon in sedimentary rocks. *Nature*, **333**, 313–318, https://doi.org/10.1038/333313a0

Schidlowski, M, Eichmann, R. and Junge, C.E. 1976. Carbon isotope geochemistry of the Precambrian Lomagundi carbonate province, Rhodesia. *Geochimica et Cosmochimica Acta*, **40**, 449–455, https://doi.org/10.1016/0016-7037(76)90010-7

Scott, C., Wing, B.A. *et al.* 2014. Pyrite multiple-sulfur isotope evidence for rapid expansion and contraction of the early Paleoproterozoic seawater sulfate reservoir. *Earth and Planetary Science Letters*, **389**, 95–104, https://doi.org/10.1016/j.epsl.2013.12.010

Shields, G.A. and Mills, B.J. 2017. Tectonic controls on the long-term carbon isotope mass balance. *Proceedings National Academy of Sciences U.S.A.*, **114**, 4318–4323, https://doi.org/10.1073/pnas.1614506114

Shields, G. and Veizer, J. 2002. Precambrian marine carbonate isotope database: version 1.1. *Geochemistry Geophysics Geosystems*, **3**, 1–12, https://doi.org/10.1029/2001GC000266

Stiller, M., Rounick, J.S. and Shasha, S. 1985. Extreme carbon-isotope enrichments in evaporating brines. *Nature*, **316**, 434–435, https://doi.org/10.1038/316434a0

Swart, P.K. 2008. Global synchronous changes in the carbon isotopic composition of carbonate sediments unrelated to changes in the global carbon cycle. *Proceedings of the National Academy of Sciences U.S.A.*, **105**, 13741–13745, https://doi.org/10.1073/pnas.0802841105

Tikhomirova, M. and Makarikhin, V.V. 1993. Possible reasons for the $\delta^{13}C$ anomaly of lower Proterozoic sedimentary carbonates. *Terra Nova*, **5**, 244–248, https://doi.org/10.1111/j.1365-3121.1993.tb00255.x

Tukey, J.W. 1958. Bias and confidence in not quite large samples. *The Annals of Mathematical Statistics*, **29**, 614, https://doi.org/10.1214/aoms/1177706647

Walther, J. 1894. *Lithogenesis der Gegenwart – Beobachtungen über die Bildung der Gesteine an der Heutigen Erdoberfläche. Dritter Theil Einer Einleitung in die Geologie als Historische Wissenschaft*. G. Fischer, Jena, 535–1055.

Wigforss-Lange, J. 1999. Carbon isotope 13C enrichment in Upper Silurian (Whitcliffian) marine calcareous rocks in Scania, Sweden. *GFF*, **124**, 273–279, https://doi.org/10.1080/11035899901214273

Yudovich, Ya.E., Makarikhin, V.V., Medvedev, P.V. and Sukhanov, N.V. 1990. Carbon isotopic anomalies in the carbonates of the Karelian Complex. *Geokhimiya*, **7**, 972–978.